

# Supporting Information

## Pulse laser deposition assisted grown continuous monolayer MoSe<sub>2</sub>

Farman Ullah, Tri Khoa Nguyen, Chinh Tam Le and Y. S. Kim\*

Department of Physics and Energy Harvest Storage Research Center,  
University of Ulsan, Ulsan 44610, S. Korea

### S1. Experimental Section

#### 1. MoO<sub>3</sub> target preparation

Approximately 13 g of pure MoO<sub>3</sub> (99.99 %, Alfa) were initially placed at 100°C to remove the moisture. The powder were ball milled in ethanol for more than 24 hours. The milled powder were dried to remove the ethanol. The powder were molded to form circular target with approximately 2 cm diameter at pressure of 5 tons. The target was annealed at 700°C for 12 hours.

#### 2. MoO<sub>3</sub> film by pulse laser deposition

The schematic illustration for continuous monolayer MoSe<sub>2</sub> by selenization of PLD deposited MoO<sub>3</sub> film is given in the Fig. S1. The growth procedure for monolayer MoSe<sub>2</sub> by PLD assisted selenization method is as follows: the chamber pressure was initially reduced to the base value  $5 \times 10^{-7}$  Torr. Highly pure MoO<sub>3</sub> target was placed in rotating target holder. The possible surface contaminants aggregated on the target were

removed by exposing the target to high energy laser beam for few minutes. The substrate was placed in a rotating substrate holder. The distance between substrate and target was set to 10 cm. A krypton fluoride (KrF) excimer laser ( $\lambda=248$  nm, CompexPro 102F) with 20 ns pulse width was used. MoO<sub>3</sub> thin films were deposited at various laser energies (given in main text) with repetition rate of 3Hz (# of laser shots on the target per second) and deposition time of 20 s. The substrate temperature was maintained at 200°C.

### **3. Selenization of MoO<sub>3</sub> films**

To convert the MoO<sub>3</sub> films to MoSe<sub>2</sub>, the deposited MoO<sub>3</sub> films were selenized in a two zones hot-wall furnace system (Fig. S1 (b)). Approximately 0.30 gram of pure selenium powder (99.99 %, Alfa) was placed in graphite crucible. The PLD deposited MoO<sub>3</sub> sample was placed 15 cm away from the selenium powder in the quartz tube. The tube pressure was reduced to the base value of 60 mtorr. Initially, pure Ar gas was flashed into the quartz tube repeatedly to clean the oxygen contaminants. The temperatures of zone-1 and zone-2 were set to 450 °C and 900 °C respectively. The tube pressure was maintained to 550 torr during the selenization process. A total 25 min reaction time was given.

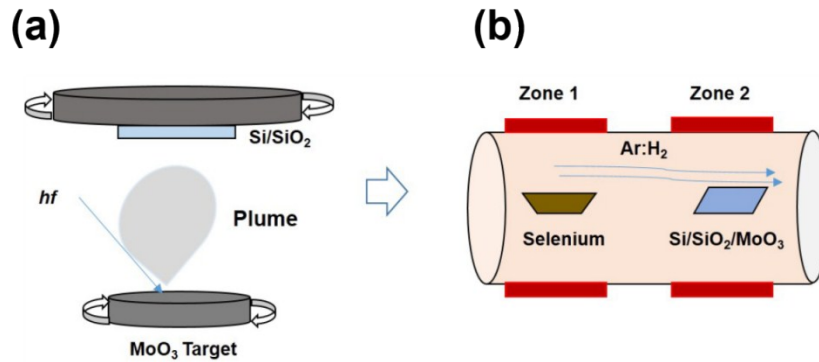


Fig. S1 . Schematic illustration of (a) pulse laser deposition system and (b) two zone furnace

#### 4. Characterization

Spectroscopic, microscopic and optical characterization were carried out to examine the grown MoSe<sub>2</sub> films. The surface morphology of the films was checked by atomic force microscopy (AFM; tapping mode with cantilever of  $k \sim 1.8$  N/m, 0.5 Hz scan speed) and field emission second electron microscopy (FE-SEM; JEOL, JSM 6500F). PL and Raman spectra's were taken at room temperature using argon Ar<sup>+</sup> laser (Melles Griot, 35-LAP-431-220) with 514.5 nm excitation light source. The spot size of laser was about  $\sim 1$   $\mu$ m. A single grating spectrometer (Princeton Instruments, SP-2500i) with a focal length of  $\sim 50$  cm was used to analyze the scattered light from the sample and was detected with a cooled liquid nitrogen CCD detector (Princeton Instruments, Spec-10). The recorded wavelength and Raman shift of the scattered light were calibrated by using the standard Neon calibration lamp (Newport, 6032). The chemical composition analysis was done by X-ray photoelectron spectroscope (XPS; Theta Probe AR-XPS System, ThermoFisher Scientific). Two-dimensional grazing incidence X-ray diffraction (2D-GIXD) measurement was conducted at the PLS-II 9A U-SAXS beamline of PAL. The X-rays coming from the in-vacuum undulator (IVU) were monochromated

(wavelength  $\lambda=0.6224 \text{ \AA}$ ) using a double crystal monochromator and focused both horizontally and vertically (FWHM  $300 \text{ \mu m}$  (H)  $\times$   $30 \text{ (V) \mu m}$  at detector position) using K-B type mirrors. Diffraction angles were calibrated by a pre-calibrated sucrose (Monoclinic, P21,  $a = 10.8631 \text{ \AA}$ ,  $b = 8.7044 \text{ \AA}$ ,  $c = 7.7624 \text{ \AA}$ ,  $\beta = 102.938^\circ$ ) and the sample-to-detector distance was about  $222 \text{ mm}$ . In-vacuum GIXD system was equipped with a 7-axis motorized sample stage for the fine alignment of thin film. GIXD patterns were recorded with a 2D CCD detector (Rayonix SX165, USA); X-ray irradiation time was  $10 \text{ s}$ .

## **S2. Thickness dependent photoluminescence and Raman scattering of MoSe<sub>2</sub>**

Although the grown MoSe<sub>2</sub> by PLD assisted method was dominantly monolayer, still regions with extra layers were also found. Mono, bi, tri and bulk areas can be identified by the thickness dependent color contrast of MoSe<sub>2</sub> on Si/SiO<sub>2</sub> substrate, as shown in Fig. S2(a). The PL and Raman spectra were taken at thick regions are shown in Fig. S2(b) and Fig. S2(c), respectively. It can be seen that PL intensity decreases exponentially with increasing thickness, indicating the transition from direct to indirect band gap. Moreover, the red shift in energy with increasing thickness can also be observed. Raman Scattering strongly depends on the number of layers. It can be seen that in monolayer region the Raman spectra show only  $A_{1g}$  and  $E_{2g}^1$ . However, at the thicker regions,  $B_{2g}^1$  vibrational mode at  $354.8 \text{ cm}^{-1}$  also appears. The intensity of  $E_{2g}^1$  peak trends to decrease with the increase of thickness. This observation is in good agreement with previous reports.<sup>1-2</sup>

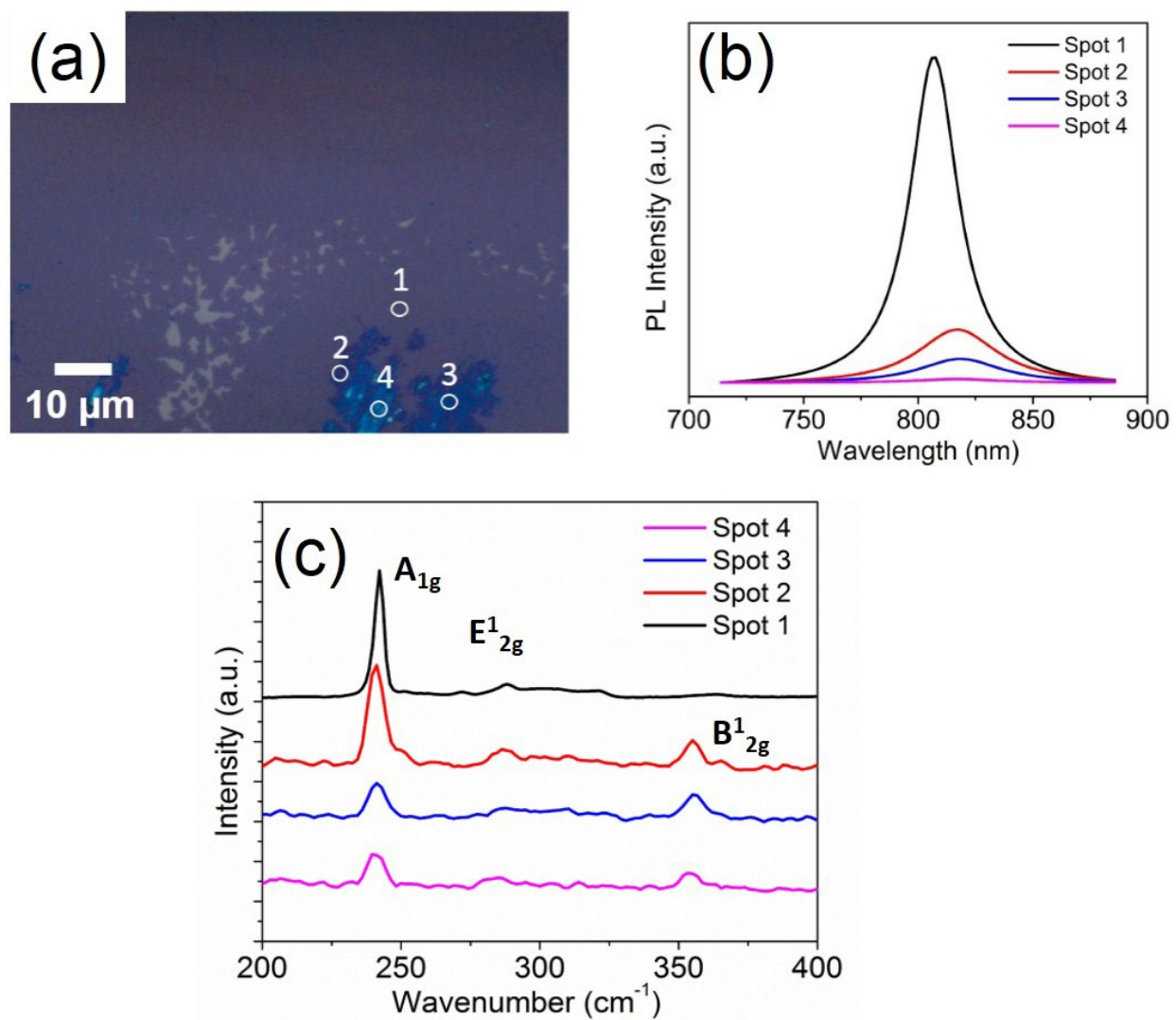


Fig. S2 (a) Optical microscope image of monolayer MoSe<sub>2</sub> with extra layers and (b) photoluminescence spectra's and (c) Raman spectra's taken on the spots in (a)

### S3. Raman and photoluminescence mapping over large area

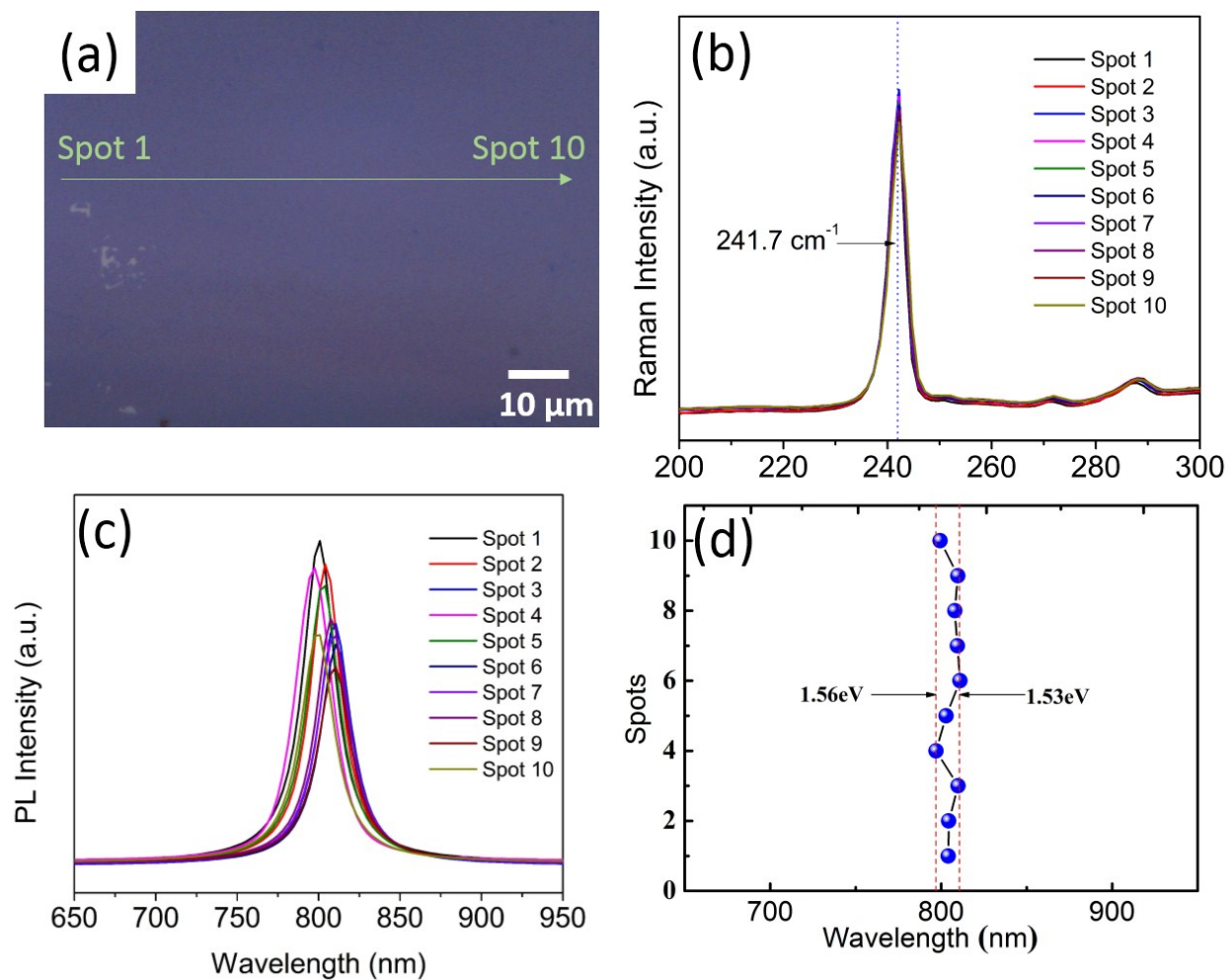


Fig. S3. (a) Optical microscope image of continuous monolayer MoSe<sub>2</sub> (c) Raman and (d) photoluminescence spectra taken at spot 1 to 10 with step size  $\sim 10 \mu\text{m}$ .

#### S4. Nonlinear characteristics of monolayer MoSe<sub>2</sub>

The highly crystalline nature of as-grown monolayer MoSe<sub>2</sub> was also confirmed by rotational angle second harmonic generation (RA-SHG) technique in our previous publication.<sup>3</sup> Owing to inversion symmetry breaking, the monolayer MoSe<sub>2</sub> could generate the SH signal. Fig. S4 shows the RA-SHG data of monolayer MoSe<sub>2</sub> flake for parallel (purple dots) and perpendicular (green dots) polarization at normal incidence scheme. The result shows clear six-petal pattern, indicating the as-grown films belong to D<sub>3h</sub> symmetry point. This implies that the as-grown films are highly crystalline monolayer MoSe<sub>2</sub>.

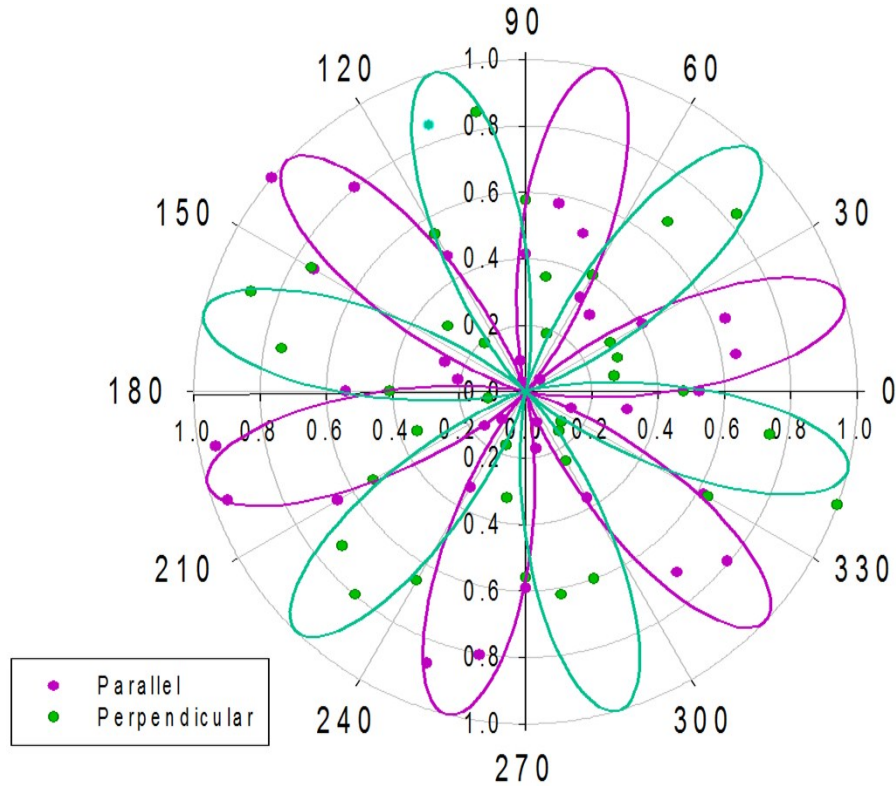


Fig.S4 Azimuthal symmetry of PLD-assisted grown MoSe<sub>2</sub> analyzed by RA-SHG . The solid traces are fit curves corresponding to  $\cos^2[3(\theta + \theta_0)]$  and  $\sin^2[3(\theta + \theta_0)]$ , where  $\theta$  denotes the angle between the incident linearly polarized electric field and the mirror axis of the crystal and  $\theta_0$  denotes the initial angular offset





## S5. MoSe<sub>2</sub> on sapphire by pulse laser deposition assisted selenization process

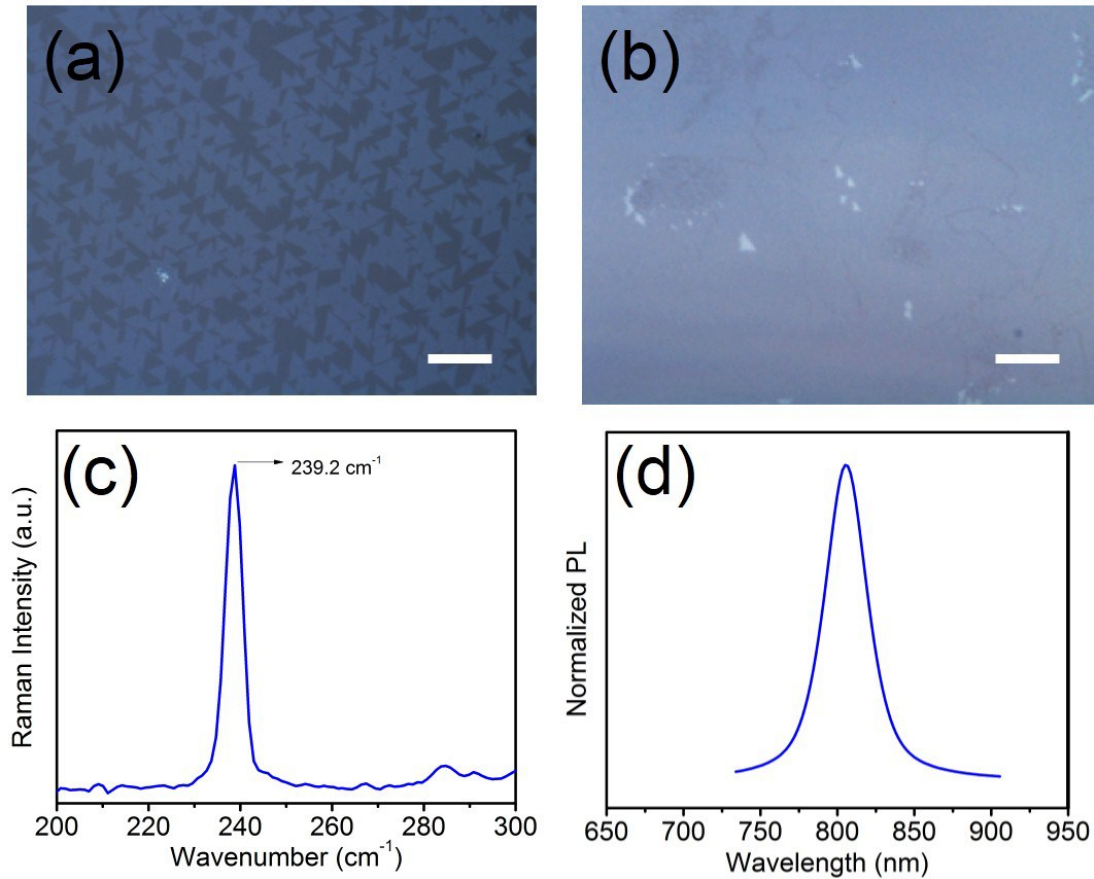


Fig. S5. Monolayer MoSe<sub>2</sub> on sapphire substrate by PLD assisted method (a) flakes (b) continuous film (c) Raman and (d) photoluminescence spectra. The scale bar is 30  $\mu\text{m}$

### Reference:

- [1] X. Lu, M.I. Utama, J. Lin, X. Gong,† J. Zhang, Y. Zhao, S.T. Pantelides, J. Wang, Z. Dong, Z. Liu, W. Zhou and Q. Xiong, *Nano Lett.* 2014, **14**, 2419-2425
- [2]. P. Tonndorf, R. Schmidt, P. Böttger, X. Zhang, J. Börner, A. Liebig, M. Albrecht, C. Kloc, O. Gordan, D. R. T. Zahn, S.M.d. Vasconcellos, and R. Bratschitsch, *Opt. Express*, 2013, **21**, 4911
- [3] C. T. Le, D. J. Clark, F. Ullah, V. Senthilkumar, J. I. Jang, Y. Sim, M. J. Seong, K. H. Chung, H. Park and Y. S. Kim, *Ann. Phys.*, 2016, DOI:10.1002/andp.201600006. (in press)